JOURNAL OF BIOLOGICAL REGULATORS & HOMEOSTATIC AGENTS Vol. 26, no. 1, 97-109 (2012)

ENDOCYTOSIS AND INTRACELLULAR LOCALISATION OF TYPE 1 RIBOSOME-INACTIVATING PROTEIN SAPORIN-S6

A. BOLOGNESI[1], L. POLITO[1], V. SCICCHITANO[1], C. ORRICO[2], G. PASQUINELLI[2], S. MUSIANI[1], S. SANTI[3], M. RICCIO[4], M. BORTOLOTTI[1] and M.G. BATTELLI[1]

[1]Department of Experimental Pathology, [2]Department of Radiological and Histopathological Sciences, Alma Mater Studiorum - University of Bologna, Bologna, Italy; [3]IGM-CNR, Unit of Bologna, c/o IOR, Bologna, Italy; [4]Department of Anatomy and Histology, University of Modena and Reggio Emilia, Modena, Italy

Received May 25, 2011 – Accepted December 21, 2011

The first two authors contributed equally to this work

Saporin-S6 is a single-chain ribosome-inactivating protein (RIP) that has low toxicity in cells and animals. When the protein is bound to a carrier that facilitates cellular uptake, the protein becomes highly and selectively toxic to the cellular target of the carrier. Thus, saporin-S6 is one of the most widely used RIPs in the preparation of immunoconjugates for anti-cancer therapy. The endocytosis of saporin-S6 by the neoplastic HeLa cells and the subsequent intracellular trafficking were investigated by confocal microscopy that utilises indirect immunofluorescence analysis and transmission electron microscopy that utilises a direct assay with gold-conjugated saporin-S6 and an indirect immunoelectron microscopy assay. Our results indicate that saporin-S6 was taken up by cells mainly through receptor-independent endocytosis. Confocal microscopy analysis showed around 30% co-localisation of saporin-S6 with the endosomal compartment and less than 10% co-localisation with the Golgi apparatus. The pathway identified by the immunofluorescence assay and transmission electron microscopy displayed a progressive accumulation of saporin-S6 in perinuclear vesicular structures. The main findings of this work are the following: i) the nuclear localisation of saporin-S6 and ii) the presence of DNA gaps resulting from abasic sites in HeLa nuclei after intoxication with saporin-S6.

Ribosome-inactivating proteins (RIPs) (1) are depurinating enzymes that are expressed in a large number of plants. These proteins have *N*-glycosidase activity that removes a specific adenine residue (A_{4324} in rat liver rRNA) from rRNA and irreversibly damages ribosomes and causes the inhibition of protein synthesis. RIPs also depurinate DNA; thus, the denomination of polynucleotide adenine glycosylase (PNAG) was proposed. These proteins are divided into type 1 and type 2 RIPs depending on the type of polypeptide chains that constitute the structure. The majority of known RIPs are single-chain proteins (type 1 RIPs). Other RIPs are galactoside-specific lectins consisting of A chain(s)

Key words: anti-cancer drugs, endocytosis, intracellular trafficking, saporin-S6, type 1 ribosome-inactivating proteins

Mailing address:
Prof. Maria Giulia Battelli,
Via S. Giacomo 14,
40126 Bologna, Italy
Tel: +39 051 2094700
Fax: +39 051 2094746
email: mariagiulia.battelli@unibo.it

0393-974X (2012)

with the same enzymatic activity as type 1 RIPs and are linked to cell binding B chain(s) with lectin properties (type 2 RIPs). Certain type 2 RIPs are potent toxins, the most well-known being ricin and abrin. Other type 2 RIPs have a similar structure and enzymatic properties but are less toxic (2-4).

The mechanism of the entry and intracellular routing of type 2 RIPs has been extensively studied, particularly the mechanism of ricin. Ricin, through the lectin chain, binds the terminal galactose or *N*-acetylgalactosamine residues of glycoproteins and glycolipids on the cell surface. After the endocytosis of ricin by clathrin-dependent and independent mechanisms, ricin is routed through the endosomal compartment to the multi-vesicular body and about 5% of the protein is sorted in the trans-Golgi network (TGN). Several lines of evidence indicate that this small amount of ricin is responsible for ricin targeting to the ribosome and cytotoxicity. Ricin reaches the endoplasmic reticulum (ER) through the retrograde transport system that mediates the routing of misfolded proteins from the TGN to the ER compartment (5). The translocation of type 2 RIPs from the ER to the cytosol has been proposed to occur in two steps: the reduction of the disulphide bridge between the A and B chains; and the cytosolic entry of the A chain using the quality control pathway that leads to ER-associated protein degradation (6, 7). The localisation of a recombinant ricin A chain fused to EGFP (enhanced green fluorescent protein) in the ER was shown by confocal microscopy and immunogold labelling electron microscopy (8).

The B chain facilitates the endocytosis of type 2 RIPs that justifies, at least in part, the higher toxicity of certain type 2 RIPs to cells and animals compared to type 1 RIPs. The toxicity of type 2 RIPs to the mouse is highly variable with a lethal dose at 50% (LD_{50}) ranging from 1μg/kg to 40μg/kg body wt, whereas the LD_{50} of type 1 RIPs ranges between 1 and 44 mg/kg (2). In particular, the type 1 RIP saporin-S6 (from *Saponaria officinalis*), hereinafter referred to as saporin, kills mice with a LD_{50} at 6 days of 4μg/kg body wt (9).

Saporin and other type 1 RIPs have been extensively used in generating immunotoxins (10, 11) to target the specific epitopes expressed on the surface of tumour or other unwanted cells. In these cases, the carrier largely mediates the binding and endocytosis of the conjugates that are responsible for selective cytotoxicity. Thus, the study of the intracellular localisation of saporin is essential for investigating a possible anti-cancer utilisation of saporin-containing immunotoxins (12).

Of note, saporin and other type 1 RIPs were shown to induce apoptotic cell death alone or as a toxic component of immunotoxins (13). Moreover, ricin and saporin were cytotoxic through more than one cell death mechanism (14). Recently, it has been shown that a saporin mutant that is unable to inhibit protein synthesis can induce apoptosis of intoxicated cells (15). Thus, RNA damage is not required to trigger apoptosis.

In previous studies, the mechanism of endocytosis and the intracellular fate of type 1 RIPs, gelonin (16-18), saporin (19-22), and trichosanthin (23, 24) were investigated. Although in some cell types a receptor-mediated endocytosis by the LDL receptor family was suggested, the interaction of type 1 RIPs with cells needs to be clarified.

In this study, we examined the endocytosis of saporin and the intracellular routing and subcellular localisation in HeLa cells by indirect immunofluorescence using a confocal microscope and direct and indirect gold staining using an electron microscope. In particular, we tried to establish whether saporin is able to enter the cell nucleus and induce DNA depurination.

MATERIALS AND METHODS

Saporin

Saporin was isolated as previously described (25) from the seeds of *Saponaria officinalis* kindly supplied by the Azienda Regionale delle Foreste della Regione Emilia Romagna, Casola Valsenio, RA, Italy. Protein purity was analysed by reverse-phase HPLC on a Vydac C4 column (Hesperia, CA, USA) as described previously (26) and was close to 99% of the total protein.

Antibodies

Rabbit anti-saporin polyclonal antibodies were prepared as previously described (27). The anti-GM130 monoclonal antibody was from BD Transduction Laboratories, Heidelberg, Germany. The anti-BiP/GRP78 monoclonal antibody was from Stressgen Biotechnology, San Diego, CA, USA. Fluorescein isothiocyanate (FITC)-

conjugated goat anti-rabbit IgG polyclonal antibodies were from Calbiochem, Darmstadt, Germany. Cy™5-conjugated donkey anti-mouse IgG polyclonal $F(ab')_2$ antibodies were from Jackson ImmunoResearch Lab. Inc., West Grove, PA, USA. Five nanometres gold-conjugated goat anti-rabbit IgG were from Nanoprobes, Yaphank, NY, USA. Gold-labelled goat anti-rabbit IgG 10 nm was from GE Healthcare, Buckinghamshire, UK.

Cells

HeLa cells were maintained in RPMI 1640 medium (Sigma-Aldrich, St. Louis, MO, USA) and supplemented with 10% heat-inactivated foetal bovine serum (FBS, Sigma-Aldrich), $2x10^{-3}$ M L-glutamine, 100 U/ml penicillin and 100 µg/ml streptomycin (Sigma-Aldrich) (hereinafter referred to as the complete medium) in humidified air with 5% CO_2 at 37°C. Cell viability was analysed before each experiment by Trypan blue dye exclusion.

Cell protein synthesis

The concentration of saporin inhibiting protein synthesis by 50% (IC_{50}) was assessed 24 h after seeding HeLa cells on 24-well plates (30,000 cells/well), as previously described (28) with minor modifications.

In the short-term experiments, the cultures were incubated in the absence or presence of 10^{-5} M saporin for 90 min at 37°C in complete medium and were pulsed for 30 min with 2 µCi/ml L-[4,5-^{3}H]leucine (85 Ci/mmol, GE Healthcare) in leucine- and serum-free RPMI 1640 containing the same saporin concentration. Cells were washed with $5x10^{-3}$ M sodium phosphate buffer, pH 7.5, containing $1.4x10^{-1}$ M NaCl (PBS) before the radiolabeled leucine incorporation was determined.

Immunofluorescence assay

HeLa cells were seeded on cover slips in 24-well plates (30,000 cells/well) in complete medium. After 24 h, cells were treated with saporin as detailed in the legend to Fig. 1.

At the end of each treatment, cells were washed three times with serum-free medium at 0°C and fixed with 1% p-formaldehyde in $1x10^{-1}$ M sodium phosphate buffer, pH 7.5, for 30 min at 30°C, washed twice with PBS and permeabilised with 1% saponin for 45 min at 30°C. After saturation with 1% bovine serum albumin (BSA, Sigma-Aldrich) in PBS (PBS/BSA) for 1 h at 30°C, cells were incubated with rabbit anti-saporin antibodies 1:8000 in PBS/BSA for 60 min at 30°C and washed and the FITC-conjugated anti-rabbit antibodies that were diluted 1:100 in PBS/BSA for 60 min at 30°C were added. Double-staining experiments were performed by incubating saporin-treated cells with rabbit anti-saporin antibodies and anti-GM130 monoclonal antibody (1:1000) or anti-BiP monoclonal antibody (1:100). The detection of primary antibodies was performed with FITC-conjugated anti-rabbit and Cy™5-conjugated anti-mouse antibodies (1:20). Finally, cover slips were mounted on glass slides using a Mowiol 4-88 (Sigma-Aldrich) solution (10% w/v) containing the anti-fade 1,4-diazobicyclo-[2.2.2]-octane (2.5% w/v, DABCO, Sigma-Aldrich) in $1x10^{-1}$ M Tris-HCl buffer, pH 8.5, and glycerol (20% v/v).

Fluorescence microscopy was performed with a Leitz Orthoplan microscope equipped with a 100 W epi-illumination and 40x and 100x objectives. Colour photomicrographs were obtained using a Kodak MDS 120 digital camera. The double immunofluorescence experiments were analysed by a Radiance 2000 confocal microscope, and the co-localisation was evaluated by using the LaserPix software (both from BioRad, Hercules, CA, USA) as already detailed (29).

Transmission electron microscopy

For electron microscopy experiments, $2x10^5$ cells were seeded in 6-well microtitre plates in 1 ml of complete medium. After 18 h, cells were treated with saporin at 37°C for the indicated time.

a) Morphological alteration of saporin-treated HeLa cells - To ascertain cell modifications induced by the RIP, HeLa cells were incubated with $1x10^{-6}$ M saporin for 20 h, washed three times with PBS, harvested with a cell scraper and centrifuged at 300x*g* for 5 min. Pelleted cells were washed twice with PBS, fixed with 4% p-formaldehyde in $1x10^{-1}$ M sodium phosphate buffer, pH 7.5, for 24 h at 4°C. The pellets were washed with $1.5x10^{-1}$ M sodium phosphate buffer, pH 7.5, postfixed in 1% buffered osmium tetroxide, dehydrated through a graded ethanol series (70-100%) and embedded in epoxy resin. Ultrathin sections were counterstained with uranyl acetate and lead citrate and observed on a transmission electron microscope (Philips 400T, Eindhoven, Netherland).

b) Saporin conjugation with colloidal gold - Saporin was conjugated to 5 nm colloidal gold particles (Nanoprobes) following the manufacturer's instructions. Briefly, $3x10^{-6}$ M saporin in $1x10^{-1}$ M carbonate/bicarbonate buffer, pH 10, was added at 1/10 v/v to colloidal gold that was previously adjusted to pH 10 with the same buffer. The mixture was gently stirred for 5 min at room temperature and after saturation with polyethylenglycol (PEG) 8000 (final concentration 1%) was ultracentrifuged at 49000x*g* for 2 h at 4°C. The loose pellet containing the conjugate was resuspended in $2x10^{-2}$ M Tris-HCl buffer, pH 7.5, containing 1% PEG 8000 and centrifuged as described above. The conjugate was stored at 4°C.

c) Pre-embedding experiments - HeLa cells were treated with $1x10^{-5}$ M saporin containing 1/10 of the 5

nm gold-saporin conjugate. After 20, 40, 60 and 120 min at 37°C, cells were harvested, fixed and processed for electron microscopy as described above.

d) Post-embedding experiments - An immunoelectron microscopy assay was performed on HeLa cells exposed to non-conjugated $1x10^{-5}$ M saporin in a continuous manner as described above. After fixing overnight with 4% p-formaldehyde and washing with $1.5x10^{-1}$ M sodium phosphate buffer, pH 7.5, the cells were dehydrated through a graded ethanol series (70-100%) and embedded in acrylic resin (Unicryl, BBInternational, England). Polymerisation was achieved by UV light at 4°C. Ultrathin sections were collected on gold grids, blocked in PBS/BSA for 15 min and incubated overnight at 4°C with a rabbit anti-saporin polyclonal antibody diluted 1:8000 in PBS/BSA. Grids were subsequently washed with PBS and incubated for 30 min at room temperature with 5 nm gold-conjugated anti-rabbit IgG diluted 1:10 in PBS/BSA. After washing with PBS and distilled water, grids were counterstained with uranyl acetate (3% in water) and lead citrate and observed in a transmission electron microscope. In a parallel experiment, rabbit anti-saporin polyclonal antibody was diluted 1:4000 in PBS/BSA followed by incubation with 10 nm gold-labelled anti-rabbit IgG diluted 1:5 in PBS/BSA.

Comet assay

HeLa cells were seeded in 6-well plates (100,000 cells/well) in complete medium 18 h before treatment with saporin 10^{-5} M for 2 h and incubated overnight at 37°C in the absence of RIP. The following day, cells were washed twice in PBS, harvested with a scraper, counted and resuspended in PBS at a concentration of 10^5 cells/ml. The cell suspension of 10 µl was quickly mixed with 100 µl of 1% LM agarose (Trevigen Gaithersburg, MD, USA) at 37°C, and 40 µl of this mixture was dropped onto a glass slide. Dried samples were lysed at 4°C for 2 h in the dark with a solution containing 2.5 M NaCl, 100 mM EDTA, 10 mM Tris-base, 1% sodium lauryl sarcosine and 1% Triton X-100. Afterwards, the samples were equilibrated for 30 min in freshly prepared FLARE™ buffer (Trevigen) containing 0.01 M HEPES-KOH, 0.1 M KCl and 0.01 M EDTA. Half of the samples were incubated for 1 h at 37°C with 40 µl *E. coli* endonuclease IV (Trevigen) that was diluted 1:75 with FLARE™ buffer containing BSA supplied by Trevigen. Subsequently, the slides were incubated for 30 min in the buffer containing 0.5 M EDTA and 0.2 M NaOH, pH 13, and subjected to electrophoresis (24 V, 300 mA) for 40 min at 4°C in the same buffer. The samples were washed twice with distilled water and fixed in 70% ethanol for 5 min. The slides were mounted as above using a Mowiol 4-88 solution (10% w/v) in $1x10^{-1}$ M Tris-HCl buffer, pH 8.5, containing glycerol (20% v/v) and DAPI (2.5% w/v).

RESULTS

Effect of saporin on protein synthesis by HeLa cells

Saporin cytotoxicity was verified by protein synthesis determination. Protein synthesis by HeLa cells was 83.8±9.2% after incubation with $1x10^{-5}$ M saporin for 120 min. The IC_{50} after 24 h incubation was $6.14x10^{-7}$ M.

Intracellular localisation of saporin by immunofluorescence analysis

The pulse-chase exposure of HeLa cells to saporin for different times at 37°C showed that the RIP was already intracellularly localised after 20 min (Fig. 1A). The FITC-conjugated anti-saporin antibody was in endocytic vesicles distributed in the cytosol. The fluorescence pattern reached and accumulated in a perinuclear vesicular structure. The small amount of staining visible in the nuclear spot could not confirm nor exclude the presence of saporin inside the nucleus.

The double immunofluorescence analysis performed by confocal microscopy showed an approximate 30% co-localisation of saporin with the endoplasmic reticulum (ER) marker BiP as demonstrated by the co-localisation binary map (Fig. 1B). After 20, 40 and 60 min of exposure to saporin, there was not a significant difference in the amount of protein that localised in the ER. A similar pattern was observed with the co-localisation analysis of saporin and the Golgi marker GM130 that showed around 7% (Fig. 1C) of the saporin localised in the Golgi apparatus. After 60 min of total incubation time, 4% of the endocytosed saporin was present in the nucleus (Fig. 1D).

Effect of saporin exposure to HeLa ultrastructure

HeLa cells exposed to $1x10^{-6}$ M saporin for 20 h were similar to untreated cells (Fig. 2A) and only a few apoptotic cells were found. However, in the vast majority of treated cells minimal organelle injury was seen; mitochondria had dilated cristae and a contracted appearance (Fig. 2B); autophagocytic vacuoles, often involving degenerated mitochondria, were a common finding as well as focal dilatation of rough ER cisternae (Fig. 2C). The Golgi apparatus

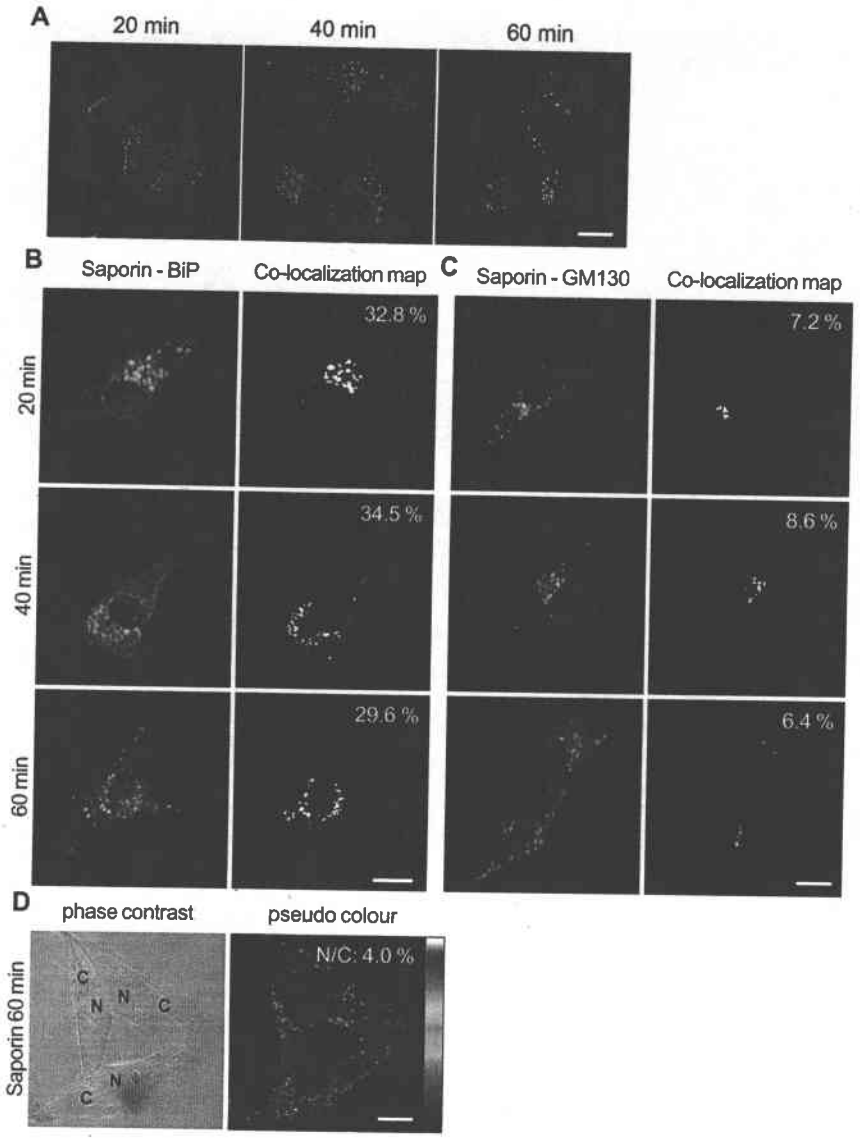

Fig. 1. *Detection of saporin by indirect immunofluorescence. HeLa cells were incubated with 10^{-5} M saporin for 20 min at 37°C, washed and incubated at 37°C up to the indicated time. Fluorescence microscopy (**A**): After fixation and permeabilisation, cells were treated with the anti-saporin polyclonal antibody and stained with the FITC-conjugated anti-rabbit antibody. Confocal microscopy and co-localisation (**B-D**): After fixation and permeabilisation, cells were treated with the anti-saporin polyclonal antibody and the anti-BiP (**B**) or anti-GM130 (**C**) antibodies. The secondary antibodies gave a green signal for saporin and a red signal for the ER (B) or Golgi apparatus (C). The percentage of co-localisation is reported together with the co-localisation binary map. **D**) The amount of saporin inside the nucleus was calculated as nuclear/cytoplasmic ratio (N/C) of grey levels and expressed as percentage. Scale bar, 10 μm.*

appeared to be well preserved.

Analysis of saporin internalisation pathway by transmission electron microscopy

The saporin internalisation pathway in the cytosolic compartment was assessed by transmission electron microscopy using pre-embedding and post-embedding procedures.

a) Experiments with gold-saporin conjugates - Time-lapse analysis of 5 nm gold-saporin complexes showed that, after 20 min of incubation, gold particles were mainly located on the plasma membrane and

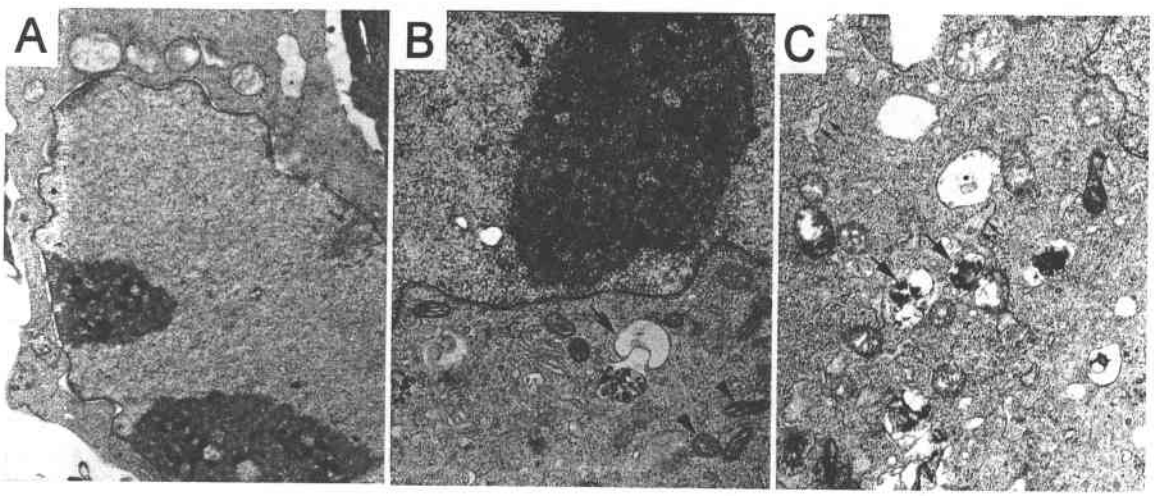

Fig. 2. *Effects of saporin on the ultrastructure of HeLa cells. Untreated HeLa cells showing normal ultrastructure (**A**). Following 20 h exposure to 10^{-6} M saporin HeLa cells show contracted mitochondria with dilated cristae (arrowheads) (**B**), numerous autophagocytic vacuoles (large arrows), often involving degenerated mitochondria, and focal dilatation of rER cisternae (small arrows) (**C**); the Golgi apparatus (G) is unaffected. Magnification: A: x9200; B: x8000; C: x11000.*

in clear vesicles and vacuoles (Fig. 3A); only in a few instances were the particles found within coated vesicles (Fig. 3B). After 40 min, gold particles were clustered in late endosomes and lysosomes in proximity to the nuclear area. Lack of gold particles in lipofuscin (Lp) suggests that gold-labelled saporin is not destined towards terminal autophagic compartment (Fig. 3C). Occasionally, clusters of gold particles were seen close to rER cisternae (Fig. 3D). The localisation of gold particles in the nuclear zone was particularly evident after 60 min (Fig. 3E) and 120 min (Fig. 3F). Interestingly, the Golgi complexes were well preserved. In control experiments, the gold-saporin complexes internalisation was inhibited by cold temperature (i.e., 4°C). Moreover, HeLa cell incubation with unconjugated-gold particles showed gold particles exclusively in the sub-plasmalemmal cytoplasmic compartment (data not shown).

b) Experiments with immunogold labelling - Comparative post-embedding analysis using a rabbit anti-saporin polyclonal antibody followed by incubation with 10 nm gold-labelled anti-rabbit IgG confirmed results from the pre-embedding procedure described above. However, after 20 min, single gold particles were observed in sub-plasmalemmal clear vacuoles and free in the cytoplasm (Fig. 4). Occasionally, after 60 min, gold particles were seen in hybrid structures formed by fusion of clear vacuoles with rER cisternae (Fig. 4E). Starting from 40 min of incubation, gold particles were seen in proximity to the nuclear envelope and within the nucleus of individual cells (Fig. 5). Nuclear localisation of saporin was present in approximately 10% of the cells; however, the gold labelling intensity varied greatly ranging from moderate (8% of HeLa cells containing less than 10 gold particles/individual nuclear area) to intense (2% of HeLa cells showing more than 10 gold particles/individual nuclear area).

Identification of DNA damage by endonuclease IV comet assay

This method relies on *E. coli* endonuclease IV that is able to detect and repair DNA gaps resulting from the recognition of abasic sites.

The chromatin of control cells was intact, which is a sign that the experimental procedure did not alter the nuclei (Fig. 6A). In more than 90% of the cases, the electrophoresis of nuclei from cells treated with saporin revealed the formation of tails, an index of DNA fragmentation (Fig. 6B). These damages are repaired in most cells by endonuclease IV, which

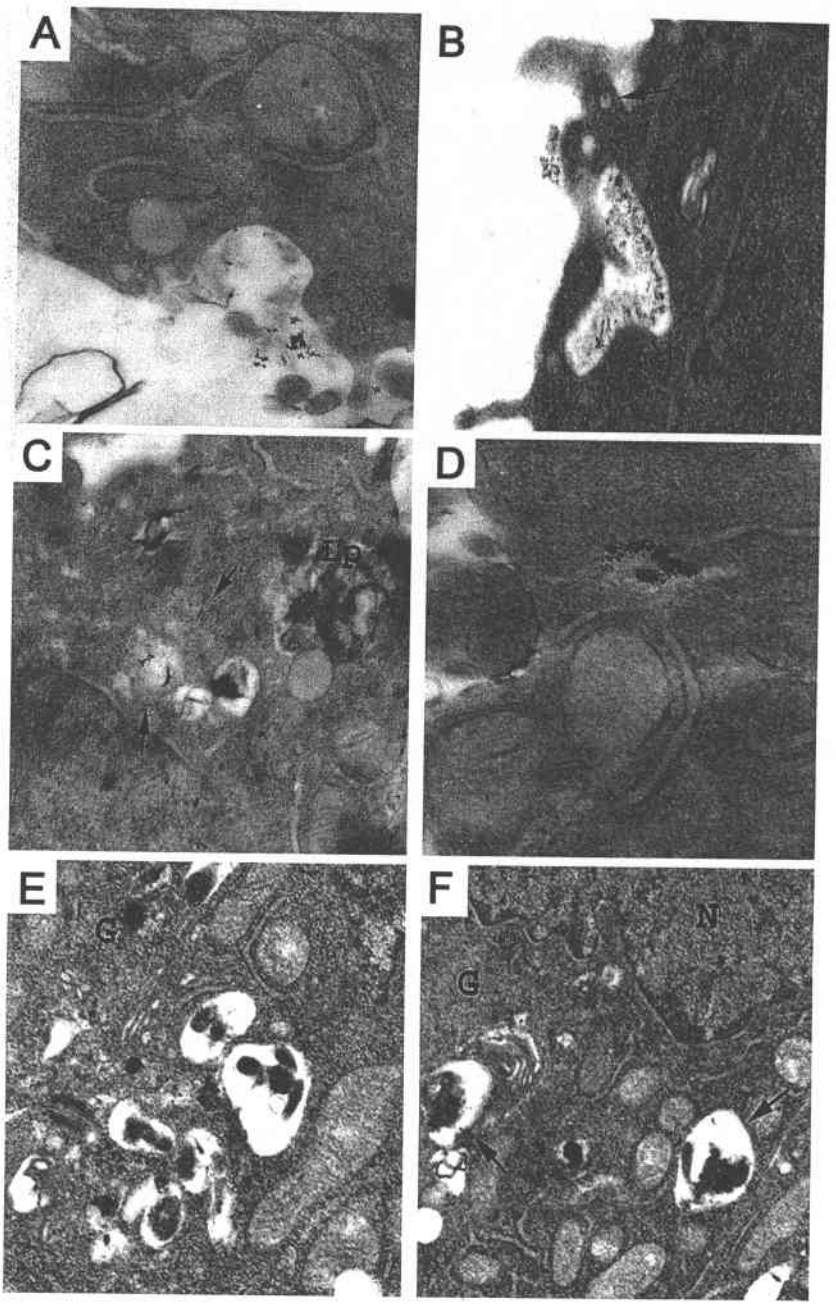

Fig. 3. *Ultrastructural analysis of saporin internalisation pathway by gold-labelled saporin. **A)** After 20 min of incubation with 10^{-5} M saporin, 5 nm gold particles are located in large invaginations of the plasma membrane; (**B**) collections of gold particles within a large pinocytotic vacuole; the arrow indicates a single gold particle in a coated vesicle; (**C**) after 40 min, clusters of gold particles (indicated by the arrows) are found in late endosomes in the Golgi zone close to the nuclear area; lipofuscin (Lp) do not contain gold particles; (**D**) occasionally clusters of gold particles are seen in close association with rER cisternae. Large collections of colloidal particles (arrows) are seen adjacent to the nuclear area after 60 (**E**) and 120 (**F**) min of incubation with 5 nm gold-saporin conjugate. The Golgi apparatus is normal-looking. Pre-embedding; 5 nm gold-saporin complexes. Magnification: x21500 (A); x36000 (B); x21500 (C); x27000 (D); x16500 (E); x13200 (F).*

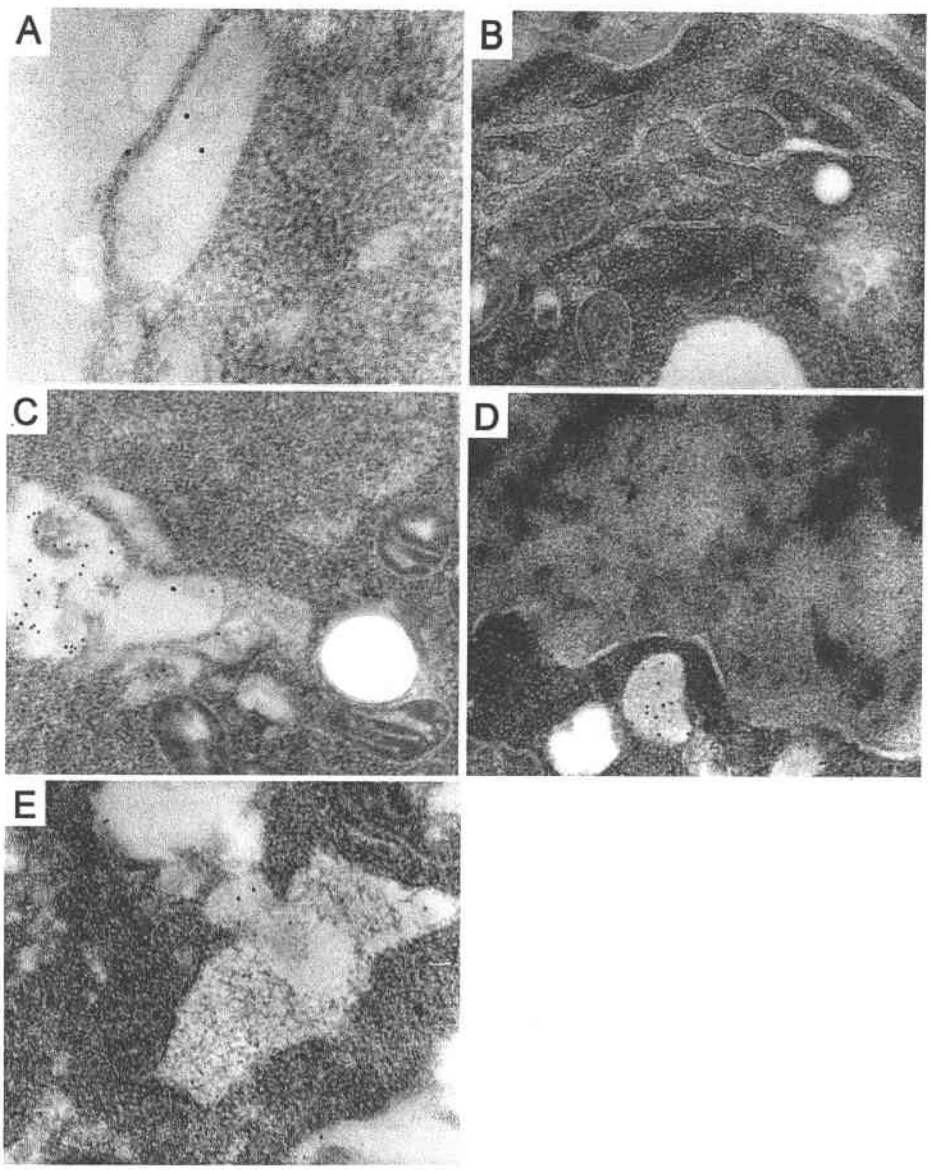

Fig. 4. *Ultrastructural analysis of saporin internalisation pathway by immunogold labelling. **A)** After 20 min of incubation with 10^{-5} M saporin, 10 nm gold particles were seen in sub-plasmalemmal clear vacuoles; **(B)** single gold particles were also observed free in the cytoplasm; **(C)** and **(D)** after 40 min, vacuoles containing gold particles were located in close proximity to the nuclear envelope; **(E)** gold particles in hybrid structures formed by fusion of clear vacuoles with rER cisternae (60 min of incubation). Post-embedding; anti-saporin polyclonal antibody followed by incubation with a 10 nm gold-labelled secondary antibody. Magnification: x46000 (A); x36000 (B, C, D); x46000 (E).*

is able to reassemble chromatin in nuclei. Less than 8% of the nuclei from saporin-treated cells appeared tailed after endonuclease IV treatment.

DISCUSSION

The present paper shows the endocytosis of saporin in HeLa cells and subsequent intracellular trafficking of saporin. This study gives detailed data for the first time regarding the full sequence of uptake and intracellular fate of type 1 RIPs. HeLa cell morphology was investigated by transmission electron microscopy. Reversible cell damage involving mitochondria, rough ER cisternae, and

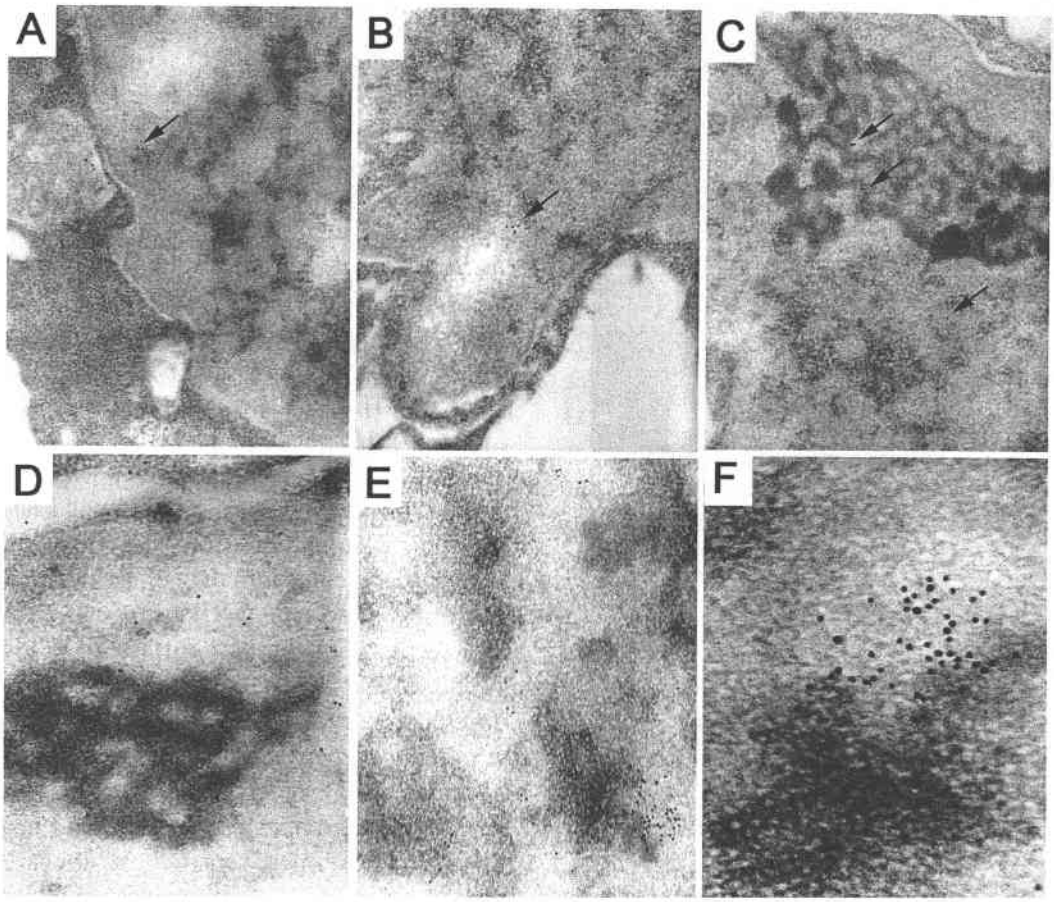

Fig. 5. *Nuclear localisation of saporin by immunogold labelling. After 40 min of saporin (10^{-5} M) treatment, individual HeLa cells showed: (**A**) isolated gold particles in a vacuole in proximity with the nucleus containing itself a single gold particle; (**B**) a few gold particles in the nucleolar zone; (**C**) some gold particles in a nucleus. In A-C the arrows indicate intranuclear gold particles. After 60 min of incubation, the number of gold particles seen in the nucleus of individual cells increased (**D-F**). Post-embedding; anti-saporin polyclonal antibody followed by incubation with a 10 nm gold labelled secondary antibody. Magnification: x16500 (A-C), x57000 (D); x38000 (E); x120000 (F).*

formation of vacuoles was observed after 20 h exposure to 10^{-6} M saporin. To study the cellular interactions of saporin and follow the progressive intracellular localisation, we used experimental conditions (10^{-5} M saporin up to 2 h) that did not result in strong inhibition of protein synthesis and visible cell alterations.

Both direct and indirect methods were utilised. Using an indirect immunofluorescence assay, the presence of saporin inside the cell was detected in the vesicular structure after only 20 min of cell exposure to the RIP. Moreover, the pulse-chase method allowed us to see saporin in vesicles that were progressively close to the nucleus. The confocal microscopy analysis confirmed the suggested intracellular routing of saporin and evaluated the co-localisation of saporin within the ER, Golgi apparatus and nucleus. However, the results of confocal microscopy did not allow us to draw a definitive intracellular pathway for saporin. For this reason, a transmission electron microscopic study was performed. To overcome any doubt about a different localisation of free and gold-conjugated saporin, direct and indirect methods were used. In the direct method, saporin was conjugated with very small gold particles (5 nm) to increase the test definition. The indirect immunoelectron microscopy assay was set up to obtain a good preservation of

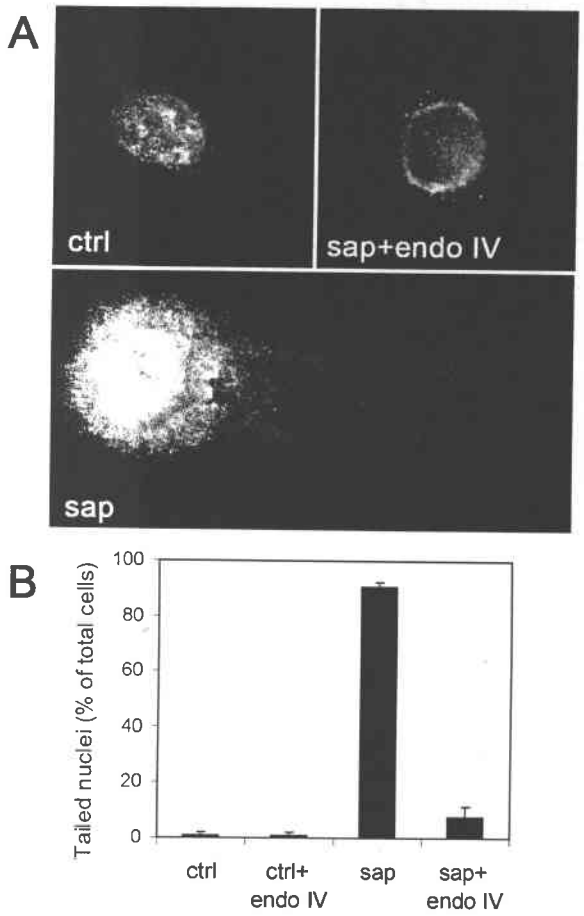

Fig. 6. *Detection of saporin enzymatic activity on cellular DNA by comet assay. HeLa cells were incubated in the absence (control cells or ctrl) or presence of saporin 10^{-5} M for 2 h and in medium without RIP overnight at 37°C (sap). Cells were prepared for the Comet assay as described in Materials and Methods. Half of the samples were incubated with endonuclease IV (ctrl+ endo IV, sap + endo IV). The slides were observed on an Eclypse E600 fluorescence microscope with a 100x immersion objective using a filter specific for DAPI (358 nm excitation λ, 461 nm emission λ).* ***A)*** *Morphology of representative nuclei.* ***B)*** *Percentage of tailed nuclei with respect to the total. Results are the means of three independent experiments with more than 100 cells counted for each slide. Standard deviations did not exceed 10%.*

cell morphology and ensure antibody recognition of saporin, i.e., the immunolabelling localisation. Finally, the evidence of a sporadic nuclear localisation of saporin prompted us to ascertain by endonuclease IV/comet assay the presence of DNA damage in intoxicated cells, possibly related to saporin depurinating activity.

Previous studies that analysed the cellular interactions of type 1 RIPs examined a single step of the sequence of events leading to cell death and could not reach conclusive indications. The first aspect examined by this study was the mechanism of saporin endocytosis. The type 1 RIP gelonin was reported to be internalised by a non-specific fluid phase pinocytosis (17, 18). Consistently, saporin uptake by HeLa cells was not due to specific binding sites (30). However, receptor-mediated endocytosis through the LDL-receptor family was concluded as a mechanism for saporin (19, 21) and another type 1 RIP, trichosanthin (23). The very low binding capacity and entry into the cell exhibited by saporin as compared to type 2 RIPs suggests a low number of receptors on the cell surface or a low binding affinity. These data confirm that this step is the foremost cause of low cytotoxicity. A discrepancy was reported between the level of α_2-macroglobulin receptor, an LDL receptor-related protein, and saporin cytotoxicity, i.e. receptor positive and negative cell lines have similar sensitivities towards saporin toxicity (31), suggesting a receptor-independent endocytosis of the RIP. The present results clearly indicate that saporin endocytosis is performed by HeLa cells mainly through non-coated vesicles.

The identification of the pathway that followed saporin entry into the endosomal compartment also needed to be clarified. Ammonium chloride, chloroquine and monensin have been utilised to study the intracellular routing of gelonin in HeLa cells (16) and saporin in haematological blasts (20). These substances had no effect on the inhibition of cell protein synthesis induced by type 1 RIPs, suggesting a lack of involvement of lysosomes and Golgi cisternae in the intracellular transport of these proteins to the cytosol. Consistent with these data, the confocal microscopy analysis showed around 30% co-localisation of saporin with the endosomal compartment and less than 10% with the Golgi apparatus. An immunofluorescence assay showed a progressive accumulation of saporin in a perinuclear vesicular structure. The pathway marked out by pre-embedding and post-embedding experiments confirmed the progression of saporin through an

endosomal vesicle to the perinuclear area. Single gold particles were observed free in the cytoplasm after only 20 min of cellular exposure to saporin and in hybrid structures formed by fusion of clear vacuoles with rER cisternae after 60 min of incubation. These data suggest that saporin reaches the cytoplasmic target by more than one mechanism. These results are in agreement with a report demonstrating that saporin, in contrast to the ricin A chain, enters the cytosol through a Golgi-independent pathway (22).

The main finding of this work is the demonstration of the nuclear localisation of saporin. Of note, this observation was obtained only with the post-embedding technique, demonstrating that the direct labelling of proteins may alter their intracellular trafficking. In addition, the nuclear localisation of saporin was observed in a limited percentage of intoxicated cells. This result is in agreement with the low percentage of nuclear localisation calculated from the confocal microscopy data. The fact that saporin may reach the nucleus raises questions about the biological meaning of the depurinating activity of RIPs on DNA, i.e., the role of this enzymatic activity on RIP cytotoxicity. The presence of saporin in the nucleus suggests that the DNA damage could be one of the mechanisms used by this protein and possibly other RIPs to kill the cell, specifically by inducing the DNA-dependent apoptotic death. The low percentage of gold-labelled nuclei also suggests that saporin utilises more than one mechanism of cell killing.

A specific comet assay was developed to further investigate the possibility that saporin, albeit in small amounts, could reach the nucleus and exert its activity on DNA. This assay was able to detect DNA gaps resulting from the detachment of purinic/pyrimidinic bases by showing DNA degradation. The addition of endonuclease IV allowed the shape recovery of the nuclei, highlighting the repair of the DNA damage due to base cleavage that could be induced by the deadenylation activity of RIP. Afterwards, a low percentage of tailed nuclei were still observed due to the incomplete action of the DNA repair system or the presence of non-recoverable breaks.

The results obtained with the comet assay indicate that saporin might be able to enter the nucleus of HeLa cells and induce DNA damage through its enzymatic PNAG activity, suggesting that the nuclear injury could be one of the mechanisms used by RIP to trigger cell death, e.g., activating DNA-dependent apoptosis (14). In this case, the action of saporin can be compared to ricin, which induced damage to nuclear DNA preceding apoptosis of endothelial cells (32).

In conclusion, our results, by showing the localisation of saporin within the ER, Golgi apparatus and nucleus, indicate that saporin reaches different subcellular compartments of HeLa cells by more than one pathway, in agreement with previous reports (20, 22). Moreover, the DNA damage apparently related to saporin depurinating activity could be one of the mechanisms of cell killing by saporin, in addition to the well-known ribosomal injury. According to previous reports (14, 15), our results suggest that saporin, and possibly other RIPs, utilises more than one mechanism to trigger cell death.

ACKNOWLEDGEMENTS

This study was supported by the University of Bologna and the Pallotti's Legacies for Cancer Research.

REFERENCES

1. Stirpe F, Battelli MG. Ribosome-inactivating Proteins: progresses and problems. Cell Mol Life Sci 2006; 63:1850-66.
2. Battelli MG. Cytotoxicity and toxicity to animals and humans of ribosome-inactivating proteins. Mini-Rev Med Chem 2004; 4:513-21.
3. Girbes T, Ferreras JM, Arias FJ, et al. Non-toxic type 2 ribosome-inactivating proteins (RIPs) from Sambucus: occurrence, cellular and molecular activities and potential uses. Cell Mol Biol (Noisy-le-grand) 2003; 49:537-45.
4. Ferreras JM, Citores L, Iglesias R, Jiménez P, Girbés T. Sambucus Ribosome-Inactivating Proteins and Lectins. Toxic Plant Proteins, Plant cell Monographs; Lord JM, Hartley MR; Eds.; Springer-Verlag: Berlin, Germany, 2010; 18:107-31.
5. Sandvig K, Grimmer S, Lauvrak SU, Torgersen ML, Skretting G, van Deurs B, Iversen TG. Pathways followed by ricin and Shiga toxin into cells. Histochem Cell Biol 2002; 117:131-41.

6. Roberts LM, Lord JM. Ribosome-inactivating proteins: entry into mammalian cells and intracellular routing. Mini-Rev Med Chem 2004; 4:505-12.
7. Lord JM, Spooner RA. Ricin trafficking in plant and Mammalian cells. Toxins 2011; 3:787-801.
8. Liu Q, Zhan J, Chen X, Zheng S. Ricin A chain reaches the endoplasmic reticulum after endocytosis. Biochem Biophys Res Commun 2006; 343:857-63.
9. Stirpe F, Gasperi-Campani A, Barbieri L, Falasca A, Abbondanza A, Stevens WA. Ribosome-inactivating proteins from the seeds of *Saponaria officinalis* L. (soapwort), of *Agrostemma githago* L. (corn cockle) and of *Asparagus officinalis* L. (asparagus), and from the latex of *Hura crepitans* L. (sandbox tree). Biochem J 1983; 216:617-25.
10. Bolognesi A, Polito L. Immunotoxins and other conjugates: pre-clinical studies. Mini-Rev Med Chem 2004; 4:563-83.
11. Kreitman RJ. Immunotoxins for targeted cancer therapy. AAPS J 2006; 8:E532-51.
12. Polito L, Bortolotti M, Pedrazzi M, Bolognesi A. Immunotoxins and other conjugates containing saporin-S6 for cancer therapy. Toxins. 2011; 3:697-720.
13. Bolognesi A, Tazzari PL, Olivieri F, Polito L, Falini B, Stirpe F. Induction of apoptosis by ribosome-inactivating proteins and related immunotoxins. Int J Cancer 1996; 68:349-55.
14. Polito L, Bortolotti M, Farini V, Battelli MG, Barbieri L, Bolognesi A. Saporin induces multiple death pathways in lymphoma cells with different intensity and timing as compared to ricin. Int J Biochem Cell Biol 2009; 41:1055-61.
15. Sikriwal D, Ghosh P, Batra JK. Ribosome inactivating protein saporin induces apoptosis through mitochondrial cascade, independent of translation inhibition. Int J Biochem Cell Biol 2008; 40:2880-8.
16. Goldmacher VS, Blattler WA, Lambert JM, McIntyre G, Stewart J. Cytotoxicity of gelonin conjugated to targeting molecules: effects of weak amines, monensin, adenovirus, and adenoviral capsid proteins penton, hexon, and fiber. Mol Pharmacol 1989; 36:818-22.
17. Madan S, Ghosh PC. Interaction of gelonin with macrophages: effect of lysosomotropic amines. Exp Cell Res 1992; 198:52-8.
18. Colaço M, Bapat MM, Misquith S, Jadot M, Wattiaux-De Coninck S, Wattiaux R. Uptake and intracellular fate of gelonin, a ribosome-inactivating protein, in rat liver. Biochem Biophys Res Commun 2002; 296:1180-5.
19. Cavallaro U, Nykjaer A, Nielsen M, Soria MR. Alpha 2-macroglobulin receptor mediates binding and cytotoxicity of plant ribosome-inactivating proteins. Eur J Biochem 1995; 232:165-71.
20. Battelli MG, Bolognesi A, Olivieri F, Polito L, Stirpe F. Different sensitivity of CD30+ cell lines to Ber-H2/saporin-S6 immunotoxin. J Drug Target 1998; 5:181-91.
21. Ippoliti R, Lendaro E, Benedetti PA, Torrisi MR, Belleudi F, Carpani D, Soria MR, Fabbrini MS. Endocytosis of a chimera between human pro-urokinase and the plant toxin saporin: an unusual internalization mechanism. FASEB J 2000; 14:1335-44.
22. Vago R, Marsden CJ, Lord JM, Ippoliti R, Flavell DJ, Flavell SU, Ceriotti A, Fabbrini MS. Saporin and ricin A chain follow different intracellular routes to enter the cytosol of intoxicated cells. FEBS J 2005; 272:4983-95.
23. Shaw PC, Lee KM, Wong KB. Recent advances in trichosanthin, a ribosome-inactivating protein with multiple pharmacological properties. Toxicon 2005; 45:683-9.
24. Zhang F, Sun S, Feng D, Zhao WL, Sui SF. A novel strategy for the invasive toxin: hijacking exosome-mediated intercellular trafficking. Traffic 2009; 10:411-24.
25. Barbieri L, Stoppa C, Bolognesi A. Large scale chromatographic purification of ribosome-inactivating proteins. J Chromatogr 1987; 408:235-43.
26. Bolognesi A, Polito L, Lubelli C, Barbieri L, Parente A, Stirpe F. Ribosome-inactivating and adenine polynucleotide glycosylase activities in *Mirabilis jalapa* L. tissues. J Biol Chem 2002; 277:13709-16.
27. Strocchi P, Barbieri L, Stirpe F. Immunological properties of ribosome-inactivating proteins and a saporin immunotoxin. J Immunol Methods 1992; 155:57-63.
28. Bolognesi A, Polito L, Farini V, et al. CD38 as a target of IB4 mAb carrying saporin-S6: design of an immunotoxin for ex vivo depletion of hematological CD38+ neoplasia. J Biol Regul Homeost Agents

2005; 19:145-52.

29. Battelli MG, Musiani S, Buonamici L, Santi S, Riccio M, Maraldi NM, Girbes T, Stirpe F. Interaction of volkensin with HeLa cells: binding, uptake, intracellular localization, degradation and exocytosis. Cell Mol Life Sci 2004; 61:1975-84.
30. Battelli MG, Montacuti V, Stirpe F. High sensitivity of cultured human trophoblasts to ribosome-inactivating proteins. Exp Cell Res 1992; 201:109-12.
31. Bagga S, Hosur MV, Batra JK. Cytotoxicity of ribosome-inactivating protein saporin is not mediated through alpha2-macroglobulin receptor. FEBS Lett 2003; 541:16-20.
32. Brigotti M, Alfieri R, Sestili P, et al. Damage to nuclear DNA induced by Shiga toxin 1 and ricin in human endothelial cells. FASEB J 2002; 16:365-72.